Acta Cryst. (1974). B30, 1452

The Crystal and Molecular Structures of *N*-Acetyl-DL-alanine-*N*-methylamide and *N*-Acetyl-L-alanine-*N*-methylamide

BY YOSHINORI HARADA AND YOICHI IITAKA

Faculty of Pharmaceutical Sciences, University of Tokyo, Hongo, Tokyo 113, *Japan*

(*Received* 5 *December* 1973; *accepted* 1 *February* 1974)

Crystals of the DL compound (DL-AANMA) grown from an acetone solution belong to the tetragonal space group $I4_1/a$ with $a=13{\cdot}81$ (3), $c=16{\cdot}50$ (3) Å (at room temperature), $Z=16$ and those of the L compound (L-AANMA) grown from a methanol solution belong to the orthorhombic space group $P2_12_12_1$ with $a=13{\cdot}87$ (7), $b=6{\cdot}98$ (4), $c=16{\cdot}29$ (8) Å, $Z=8$. The structure of DL-AANMA was solved by the method of symbolic addition and refined by the full-matrix least-squares procedure based on the diffractometer data obtained at -137°C. The final R value was 0·072 allowing for the anisotropic thermal vibrations for each atom and for the disorder of the structure. The structure of L-AANMA was derived from that of DL-AANMA and refined by the full-matrix least-squares method based on the photographic data. The final R value was 0·12 assuming isotropic thermal vibrations for each atom. The φ_{CN} and ψ_{CC} values of the L molecules found in both crystals deviate, from those of the ideal straight-chain conformation, to the right in the Ramachandran plot, resulting in a right-hand twist of the peptide chain. In both crystals, the molecules are hydrogen-bonded, as in the β-pleated sheet structure, but the sheet is twisted to form a left-hand helical unit (for L-molecules) along the c axis. The helical unit in L-AANMA is derived from the antiparallel-chain pleated sheet while that in DL-AANMA from the parallel-chain pleated sheet. In the latter unit, about 10% of the antiparallel chains are mixed, giving rise to disorder in the structure.

Introduction

In the course of a study on infrared spectra of crystalline *N*-acetyl-alanine-*N*-methylamide, $CH_3CONHCHCH_3CONHCH_3$, Koyama, Shimanouchi, Sato & Tatsuno (1971) found two crystalline modifications, forms I and II. These two forms differ in their skeletal vibrations, as shown by the differences in the frequencies of the amide IV*a* and VI*a* bands. This paper describes the result of the crystal structure determinations of form I of both *N*-acetyl-DL-alanine-*N*-methylamide (DL-AANMA) and *N*-acetyl-L-alanine-*N*-methylamide (L-AANMA).

Experimental

The crystals of DL-AANMA and L-AANMA were grown from acetone and methanol solutions respectively. For both compounds they are transparent colourless prisms elongated along the c axis. The density was measured by the flotation method in a mixed solution of dichloroethane and benzene. Lattice constants and intensity data of DL-AANMA were obtained on a Rigaku four-circle X-ray diffractometer at room temperature and later at -137°C. In the latter case, the specimen was cooled by blowing evaporated liquid nitrogen from a Dewar vessel and the temperature was measured by a copper-constantan thermocouple placed very near the specimen. Intensities were measured by the ω–2θ scanning method with a scan speed of $4°\,2\theta$ min^{-1}. The background was measured at both sides of each diffraction peak for 10 s.

In the case of L-AANMA, although the crystals were well developed prisms in appearance, c axis Weissenberg photographs showed an elongation of the spots in a horizontal direction indicating that the crystal is composed of fragments aligned along **c** but disoriented in the perpendicular direction. The angular divergence was estimated from the lengths of the spots to be about 10° around the c axis. Trials to find better crystals were not successful and the intensities were recorded by the multiple-film method on equi-inclination Weissenberg photographs for the layers 0 and 1 around the a axis and 0 to 6 around the c axis. Because of the disorientation and the large temperature factor of the crystal, the intensities faded out rapidly in the high-angle region.

Crystal data and the intensity-data measurements are summarized in Table 1.

Determination of the structures

DL-*AANMA*

The structure was solved by the symbolic addition method (Karle & Karle, 1966) with the room-temperature data. The refinement was carried out by the block-diagonal least-squares method. During the refinement a difference Fourier map was calculated which revealed, besides a few unexplained peaks, eight hydrogen atoms out of twelve contained in an asymmetric unit. The R value was reduced to 0·08 when anisotropic temperature factors were assigned to the heavy atoms and isotropic ones to the hydrogen atoms. The bond lengths and angles, however, revealed some unexpected

values, mostly for the amide groups. A difference Fourier map calculated with the final set of parameters still showed a few unexplained peaks of about 1 e Å^{-3} near the amide groups, but it was not possible to interpret the peaks as hydrogen atoms. The situation was not improved when the refinement was carried out with the low-temperature data.

On completion of the structure determination of L-AANMA, we discovered that the structural unit in L-AANMA is very similar to that in DL-AANMA. They differ in that while the L-structural unit in DL-AANMA has 4_3 symmetry, the unit in L-AANMA has 2_1 symmetry and the two crystallographically independent molecules, M_1 and M_2, are arranged alternately. Of particular interest was the orientation of M_2, which is the reverse of that expected for the molecule related to M_1 by 4_3 symmetry. This attracted our attention and we tried to refine the structure of DL-AANMA assuming that a molecule, designated M_{rev}, was in the reverse orientation, as shown in Fig. 1.

Refinement was further continued for the disordered structure in which a fraction of the molecule M_{rev} was superposed on the molecule M. The atomic parameters of M_{rev} were obtained by rotating M through an angle of 180° about C(3) (α-carbon) while the positions of the terminal carbon atoms remain unchanged; a small adjustment of the coordinates was necessary to explain the spurious peaks in the difference Fourier map. Several sets of full-matrix least-squares refinement were then calculated based on the low-temperature intensity data. In each set the atomic parameters and the occupancy factor of M_{rev} were fixed, but the latter was increased stepwise by 0·01 from set to set. The minimum value of R, 0·072, was obtained when the occupancy factor reached 0·1. The weight function used for the calculation was:

$$\sqrt{w}=F_o/20, \text{ when } F_o<20,$$
$$\sqrt{w}=1, \text{ when } 20\leq F_o\leq 300,$$
$$\sqrt{w}=1/\{1+0{\cdot}02(F_o-300)\}, \text{ when } F_o>300.$$

The final atomic parameters for M and M_{rev} are given in Table 2. A comparison of the observed (at −137 °C) and calculated structure factors is shown in Table 3.

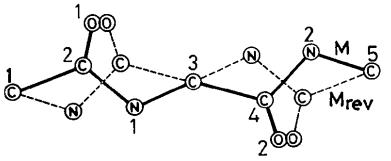

Fig. 1. Superposition of M_{rev} on the molecule of M assumed for the disordered structure of DL-AANMA.

L-*AANMA*

An interesting correlation involving the lattice constants and space-group symmetries (shown in Fig. 2) for the crystals of DL-AANMA and L-AANMA led us to suppose that a structural unit found in DL-AANMA about the 4_3 axis would also exist in L-AANMA about the 2_1 axis. Indeed, the infrared spectra observed for both crystals were so alike that a similar conformation and a similar environment of the molecules were suggested for L-AANMA. An R map was therefore calculated for the 151 strongest three-dimensional reflexions in the low 2θ-angle region. The starting model was constructed by assuming the same molecular structure

Table 1. *Crystal data and measurement of intensity data*

N-Acetyl-DL-alanine-*N*-methylamide (DL-AANMA)
N-Acetyl-L-alanine-*N*-methylamide (L-AANMA) $C_6H_{12}N_2O_2$, M.W. 144·2

	DL-AANMA		L-AANMA
	At room temperature	At −137 °C*	
Crystal system	Tetragonal		Orthorhombic
Space group	$I4_1/a$		$P2_12_12_1$
a (Å)	13·81 (3)	13·615 (10)	13·87 (7)
b (Å)	13·81 (3)	13·615 (10)	6·98 (4)
c (Å)	16·50 (3)	16·435 (10)	16·29 (8)
U (Å)^3	3144	3046·5	1579
U/molec. (Å^3)	196·5	190·41	197·4
D_m (g cm^{-3})	1·216		1·216
D_x (g cm^{-3})	1·219		1·214
Z	16		8
Intensity measurement	Diffractometer		Weissenberg camera
Radiation	Ni-filtered Cu $K\alpha$		Ni-filtered Cu $K\alpha$
Number of reflexions observed	812	811	372
% of the total	60	60	34
2θ less than	130°	130°	80°
Overall B (Å^2) (from Wilson plot)	4·5	2·6	6·9

* The specimen was not identical with that used for the room-temperature measurement though the conditions of crystallization were the same.

Table 2. *Final atomic parameters for* DL-*AANMA at* −137°C

Temperature factors are of the form $T=\exp[-(\beta_{11}h^2+\beta_{22}k^2+\beta_{33}l^2+2\beta_{12}hk+2\beta_{13}hl+2\beta_{23}kl)]$. All parameters are multiplied by 10^4 except for B, and the e.s.d.'s are given in parentheses denoting the least significant digits.

	x	y	z	β_{11}	β_{22}	β_{33}	β_{12}	β_{13}	β_{23}
M (occupancy factor = 0·9)									
C(1)	1535 (4)	1659 (5)	1764 (3)	32 (4)	49 (4)	18 (3)	0 (3)	−4 (2)	1 (2)
C(2)	1704 (5)	947 (6)	2496 (4)	25 (4)	49 (5)	24 (3)	−9 (4)	4 (3)	−10 (3)
C(3)	1642 (5)	−704 (4)	2954 (4)	47 (4)	21 (4)	26 (3)	5 (3)	−7 (3)	−3 (2)
C(4)	2666 (6)	−986 (5)	3182 (4)	68 (6)	11 (4)	27 (3)	−8 (4)	−20 (3)	1 (3)
C(5)	3811 (5)	−1656 (5)	4161 (4)	51 (5)	44 (4)	32 (3)	11 (4)	−15 (3)	4 (3)
C(6)	1036 (7)	−1611 (7)	2744 (5)	76 (7)	65 (6)	39 (4)	−20 (5)	−16 (4)	10 (4)
N(1)	1558 (4)	31 (4)	2362 (3)	45 (4)	34 (4)	21 (3)	3 (3)	6 (2)	1 (2)
N(2)	2870 (5)	−1305 (4)	3914 (3)	54 (4)	48 (4)	24 (3)	1 (3)	−2 (3)	−3 (2)
O(1)	1923 (4)	1274 (3)	3166 (2)	54 (3)	44 (3)	11 (2)	−7 (3)	−9 (2)	−3 (2)
O(2)	3355 (4)	−1002 (4)	2625 (3)	75 (4)	64 (4)	20 (3)	−3 (3)	13 (2)	9 (2)

Table 2 (*cont.*)

M_{rev} (occupancy factor = 0·1)

All parameters are assumed values except for the occupancy factor.

C(11)	3811	−1656	4161	$B=3·5$ Å^2
C(12)	3234	−1241	3425	3·5
C(13)	1642	−704	2954	3·5
C(14)	1718	382	2774	3·5
C(15)	1535	1659	1764	3·5
C(16)	584	−976	3114	3·5
N(11)	2265	−1067	3619	3·5
N(12)	1520	620	2000	3·5
O(11)	3558	−1074	2719	3·5
O(12)	1944	999	3310	3·5

Table 3. *Observed and calculated structure factors of* DL-*AANMA*

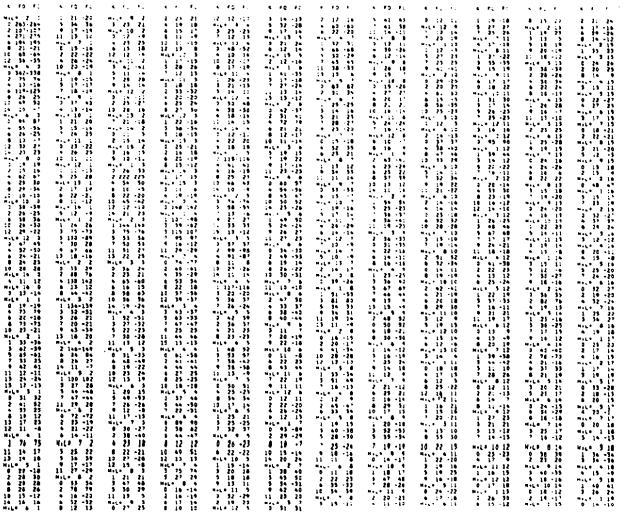

and the same relationship to the screw axis as found for M in the crystal of DL-AANMA. The molecule was then rotated around the 2_1 axis through an angle of $\pi/2$ at intervals of 0·05 rad. In each case, the molecule was translated along the c axis from $z=0$ to 0·5 at intervals of 0·02 (0·32 Å). In this calculation, although there is no need to assume the equivalence of the two successive molecules along the 2_1 axis, it was assumed that they were still in positions related by a 4_3 symmetry.

A plausible structure obtained from the R map gave a minimum R value of 0·36. This structure was then refined in the usual way by the least-squares method. In the course of the refinement, it became clear that the model could not be refined beyond the R value of 0·23 and that it also gave unreasonable bond lengths and angles. A difference Fourier map showed some unusual features which were interpretable as being one of the two crystallographically independent molecules about the 2_1 axis replaced by the molecule having the reversed orientation. This structure could be refined by the full-matrix least-squares method to an R value of 0·12 excluding hydrogen atoms. In this calculation, only individual isotropic thermal parameters were assumed because of the limited number of reflexions in the high-angle region. The weighting function was:

$$\sqrt{w}=F_o/10, \quad \text{when } F_o<10,$$
$$\sqrt{w}=1, \quad \text{when } 10\le F_o\le 30,$$
$$\sqrt{w}=1/\{1+0·02(F_o-30)\}, \quad \text{when } F_o>30.$$

The final atomic parameters are listed in Table 4 and the observed and calculated structure factors in Table 5.

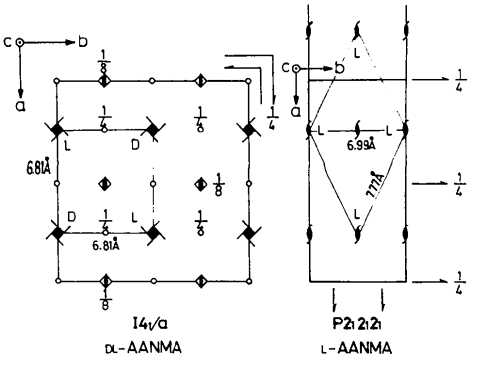

Fig. 2. Comparison of the space-group symmetries between the crystals of DL- and L-AANMA. D and L denote the helical units consisting of D and L molecules respectively. In each unit, the helix axis is coincident with the crystallographic tetrad or diad screw axis.

Table 4. *Final atomic parameters for* L-*AANMA*

		x	*y*	*z*	*B*
M_1					
	C(1)	563 (24)	1200 (52)	8176 (24)	4·6 (1·0)
	C(2)	1313 (34)	1154 (64)	7505 (34)	7·2 (1·2)
	C(3)	2944 (27)	2011 (54)	7040 (24)	4·8 (1·0)
	C(4)	3372 (29)	−87 (70)	6822 (30)	7·6 (1·3)
	C(5)	4320 (29)	−2146 (61)	5882 (25)	6·5 (1·2)
	C(6)	3689 (27)	3174 (51)	7373 (27)	5·9 (1·1)
	N(1)	2198 (23)	1656 (40)	7702 (20)	4·8 (0·8)
	N(2)	3807 (21)	−297 (45)	6092 (22)	5.2 (0·9)
	O(1)	1047 (18)	901 (37)	6750 (21)	6·5 (0·8)
	O(2)	3424 (19)	−1370 (44)	7368 (19)	7·6 (0·9)
M_2					
	C(11)	3526 (22)	3635 (46)	3516 (21)	3·4 (0·9)
	C(12)	3057 (38)	2729 (69)	4261 (37)	10·1 (1·5)
	C(13)	1555 (26)	981 (52)	4745 (25)	5·8 (1·1)
	C(14)	1851 (38)	−1117 (76)	4826 (38)	9·8 (1·5)
	C(15)	1760 (29)	−3888(62)	5758 (28)	8·3 (1·3)
	C(16)	584 (31)	1475 (59)	4455 (25)	8·3 (1·3)
	N(11)	2163 (25)	1919 (42)	4077 (24)	6·6 (0·9)
	N(12)	1655 (28)	−1716 (57)	5551 (27)	11·1 (1·3)
	O(11)	3312 (17)	2592 (40)	5042 (20)	7·4 (0·7)
	O(12)	2313 (17)	−2175 (36)	4307 (17)	7·3 (0·9)

Table 5. *Observed and calculated structure factors of* L-*AANMA*

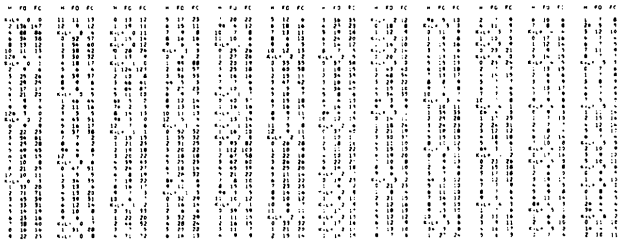

Discussion of the structure

Molecular structure

Bond lengths and angles of the AANMA molecules found in the DL and L crystals are compared in Table 6. In general the values agree, but because of the disorder in the crystal of DL-AANMA and because of the large temperature factors in addition to the poor quality of the observed F's in L-AANMA, the accuracy in the present structure determination is not high enough to make detailed comparison of the AANMA molecules possible.

The conformations of the four kinds of molecules, M and M_{rev} in DL-AANMA (we shall consider only the L molecules in the following discussion), and M_1 and M_2 in L-AANMA are essentially the same and show the distorted β pleated-sheet conformation in proteins. Various torsion angles are listed in Table 7 and the φ,ψ values are plotted on the φ–ψ chart (Ramachandran, Ramakrishnan & Sasisekharan, 1963) shown in Fig. 3. It is seen that they fall within the upper right part of the allowed region for the β structure. The planarities of the peptide groups are shown in Table 8 and the dihedral angles at the C^α atom between the two peptide planes are listed in Table 7 together with other parameters characterizing the structure of peptides. The dihedral angles in the AANMA molecules are much larger than those found in other polypeptide molecules, suggesting that the AANMA molecules are more strongly folded, although the distances between the terminal carbon atoms which correspond to the repeat distance of the peptide backbone do not differ very much from the normal value. This is en-

Table 6. *Bond lengths and angles*

	DL-AANMA (at −137 °C)		L-AANMA		Peptide
	M	M_{rev}(assumed)	M_1	M_2	model*
Bond lengths (Å)					
C(1)–C(2)	1·562 (9)	1·549	1·51 (6)	1·51 (3)	1·53
C(2)–N(1)	1·282 (9)	1·378	1·32 (6)	1·40 (4)	1·32
C(2)–O(1)	1·225 (8)	1·262	1·30 (6)	1·32 (3)	1·24
C(3)–C(4)	1·494 (10)	1·512	1·62(6)	1·53 (4)	1·53
C(3)–C(6)	1·525 (11)	1·510	1·43 (5)	1·47 (6)	
C(3)–N(1)	1·400 (8)	1·469	1·52 (5)	1·53 (4)	1·47
C(4)–N(2)	1·310 (9)	1·340	1·34 (6)	1·28 (4)	1·32
C(4)–O(2)	1·311 (9)	1·256	1·26 (6)	1·29 (3)	1·24
C(5)–N(2)	1·426 (9)	1·467	1·51 (5)	1·56 (6)	1·47
Bond angles (°)					
N(1)–C(2)–C(1)	116·6 (0·6)	111·6	117 (4)	112 (1)	114
N(1)–C(2)–O(1)	123·1 (0·7)	121·1	122 (4)	115 (1)	125
C(1)–C(2)–O(1)	120·2 (0·6)	127·3	120 (4)	133 (2)	121
C(4)–C(3)–C(6)	110·7 (0·6)	109·8	110 (3)	120 (3)	
N(1)–C(3)–C(6)	112·2 (0·6)	109·8	109 (3)	100 (3)	
N(1)–C(3)–C(4)	115·7 (0·5)	115·8	105 (3)	109 (2)	111
N(2)–C(4)–C(3)	120·9 (0·6)	114·1	117 (4)	110 (2)	114
N(2)–C(4)–O(2)	119·0 (0·6)	123·6	121 (4)	121 (2)	125
C(3)–C(4)–O(2)	119·8 (0·6)	122·3	121 (4)	129 (2)	121
C(2)–N(1)–C(3)	124·3 (0·6)	116·0	121 (3)	121 (1)	123
C(4)–N(2)–C(5)	124·3 (0·6)	118·8	120 (3)	120 (3)	123

* Pauling & Corey (1953).

tirely due to deformation of the backbone conformation which can be seen in their φ and ψ values. A similar deformation characterized by the deviation of φ, ψ values from those of the ideal straight chain (number of residues per turn, $n=2$) to the right in the Ramachandran plot is often observed in the β pleated sheets in globular proteins, as indicated recently by Chothia (1973), who has also shown that the deformation causes the polypeptide chain to twist in a clockwise direction when viewed along the chain and that the chains with such a right-hand twist are energetically more favoured than those without twist or with a left-hand twist. It is interesting to see that even such a small polypeptide as AANMA, having only one amino acid residue with two peptide groups, exhibits a tendency to take a right-hand twist. Furthermore, the deviations of the φ, ψ values from the line $n=2$ and hence the twist of the chain are much more exaggerated in AANMA than in the globular proteins mentioned by Chothia. As a result of the large deviations, the conformation of the molecules of AANMA resembles more that of polyglycine II or collagen, as shown in Fig. 4.

Crystal structure

Figs. 5 and 6 are perspective drawings of the structural units in DL- and L-AANMA drawn by the *ORTEP* program (Johnson, 1965). In these units, the molecules are arranged in such a way that the hydrogen-bonded sheets similar to the β pleated sheets are twisted to form a helical unit along the c axis, the long axis of the molecules being nearly perpendicular to the helix axis. In DL-AANMA, the D and L molecules form different units mutually antipodal and arranged as shown in Fig. 2.

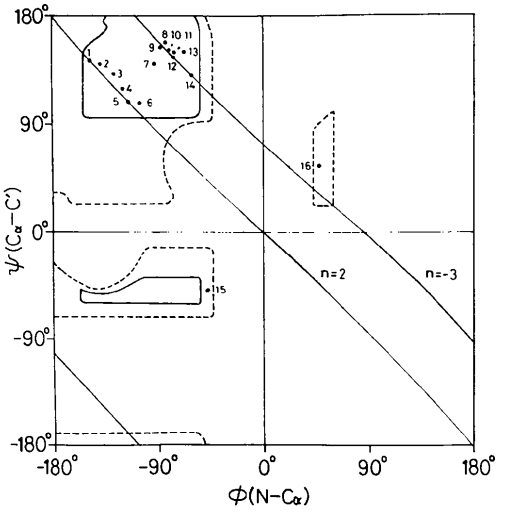

Fig. 3. The Ramachandran plot showing the backbone conformation of various peptides. The solid line encloses the fully allowed regions and broken line outer-limit regions. Contours of constant n (number of residues per turn) represent the conformations having the same n values. The right-hand helices take the positive n. (1) Antiparallel chain pleated sheet (Pauling & Corey, 1953); (2) Poly-L-alanine (Marsh, Corey & Pauling, 1955); (3) Glycylphenylalanylglycine (Marsh & Glusker, 1961); (4) *N*-Acetyl-DL-α-amino *n*-butyric acid-*N*-methylamide (Koyama, Shimanouchi, Sato & Tatsuno, 1971); (5) Parallel chain pleated sheet (Pauling & Corey, 1953); (6) *N*-Acetyl-DL-phenylalanine-*N*-methylamide (Harada & Iitaka, 1974); (7) *N*-Acetyl-DL-leucine-*N*-methylamide (Ichikawa & Iitaka, 1969); (8) *N*-Acetyl-L-alanine-*N*-methylamide(M_1) (present study); (9) *N*-Acetyl-L-alanine-*N*-methylamide(M_2) (present study); (10) *N*-Acetyl-DL-alanine-*N*-methylamide (M_{rev}) (present study); (11) *N*-Acetyl-DL-alanine-*N*-methylamide (M) (present study); (12) Polyglycine II (Crick & Rich, 1955); (13) *N*-Acetyl-glycine-*N*-methylamide (Iwasaki, 1972); (14) Collagen helix (Sasisekharan, 1962); (15) Right-handed α-helix (Pauling & Corey, 1951); (16) Left-handed α-helix.

Table 7. *Torsion angles and distortions in hydrogen bonds*

	DL-AANMA*		L-AANMA		Poly-L-alanine	ACP	PCP	Polyglycine II	Collagen
	M	M_{rev}	M_1	M_2					
φ	−75·9°	−80·5°	−84·3°	−87·6°	−139·5°	−145°	−119°	−77°	−62°
ψ	150·1	152·0	159·0	154·8	140·5	142	113	145	131
ω_1	−177·7	−177·9	−168·4	−178·2	−176·3	180	180	179	
ω_2	175·3	177·9	173·3	171·9	−176·3	180	180	179	
θ	86·3	86·8	94·2	85·3	43·3	43·5	63·5	90·1	
C(1)–C(5)	6·75 Å	6·75 Å	6·82 Å	6·85 Å	6·95 Å	7·00 Å	6·5 Å	6·5 Å	
O···N	2·94	2·9†	2·80	2·92	2·77	2·76	2·82	2·77	
	2·80	2·7†	2·73	2·72	2·77				
∠(O=C···N)	21·4°	16°	33·6°	29·5°	1·2°	1°	17°	5°	
	34·6	31	29·8	32·7	1·2				
∠(C=O···N)	149·7	156	131·6	138·3	178·2	178	156	173	
	130·0	134	136·2	132·4	178·2				
References	(1)		(2)		(3)	(4)	(5)	(6)	(7)

* For L molecules
† Between M_{rev} molecules

$\varphi = \tau$[C(2)–N(1)–C(3)–C(4)] $\quad \psi = \tau$[N(1)–C(3)–C(4)–N(2)]
$\omega_1 = \tau$[C(1)–C(2)–N(1)–C(3)] $\quad \omega_2 = \tau$[C(3)–C(4)–N(2)–C(5)]

θ: Dihedral angle between the peptide groups I and II
C(1)–C(5): Distance between C(1) and C(5) or the chain repeat distance

References: (1), (2) Present study; (3) Marsh, Corey & Pauling (1955); (4), (5) Pauling & Corey (1953); (6) Crick & Rich (1955); (7) Sasisekharan (1962).

Of particular interest is that (*a*) while the unit in DL-AANMA is derived by twisting the parallel-chain pleated sheet (PCP), that in L-AANMA is derived by twisting the antiparallel-chain pleated sheet (ACP), and (*b*) the hydrogen bonds connecting the two successive molecules are equally well formed, as shown in Figs. 5 and 6. The energy difference between the PCP and ACP structures may not be large, since the structures of DL- and L-AANMA show a close resemblance and since a fraction of the ACP structure is mixed in the crystal of DL-AANMA.

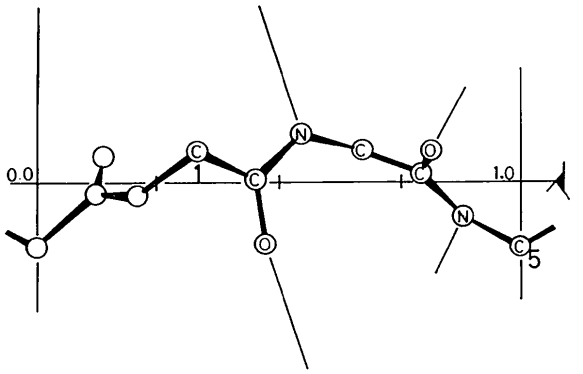

Fig. 4. Structure of polyglycine II showing a similar backbone conformation to that of L-AANMA. Two successive residues ($C_1 \sim C_5$) can be compared with the L-AANMA molecule shown at the top of Fig. 6. The six hydrogen bonds involved in one turn of the polyglycine helix link the six surrounding helices respectively to form a crystalline fibre.

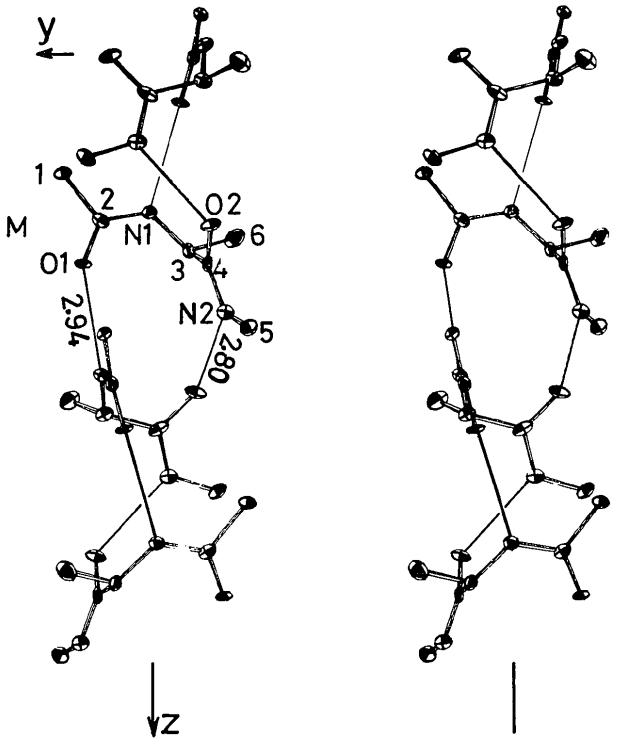

Fig. 5. A stereoscopic drawing of the helical unit of L molecules found in DL-AANMA viewed along the *a* axis. The atoms are drawn with 13% probability ellipsoids. Hydrogen bonds are shown as single thin lines.

Table 8. *Least-squares planes through the peptide groups*

DL-AANMA
Molecule *M*

Peptide group I: (1) C(1), C(2), C(3), N(1), O(1)
(2) 0·012 (3) $0{\cdot}965X-0{\cdot}103Y-0{\cdot}241Z=1{\cdot}099$
Peptide group II: (1) C(3), C(4), C(5), N(2), O(2)
(2) 0·024 (3) $0{\cdot}233X+0{\cdot}935Y+0{\cdot}266Z=0{\cdot}942$

Molecule M_{rev}

Peptide group I: (1) C(11), C(12), C(13), N(11), O(11)
(2) 0·011 (3) $0{\cdot}227X+0{\cdot}935Y+0{\cdot}274Z=0{\cdot}954$
Peptide group II: (1) C(13), C(14), C(15), N(12), O(12)
(2) 0·013 (3) $0{\cdot}965X-0{\cdot}104Y-0{\cdot}241Z=1{\cdot}097$

L-AANMA
Molecule M_1

Peptide group I: (1) C(1), C(2), C(3), N(1), O(1)
(2) 0·06 (3) $0{\cdot}237X+0{\cdot}963Y+0{\cdot}128Z=1{\cdot}15$
Peptide group II: (1) C(3), C(4), C(5), N(2), O(2)
(2) 0·04 (3) $0{\cdot}869X-0{\cdot}338Y+0{\cdot}362Z=8{\cdot}13$

Molecule M_2

Peptide group I: (1) C(11), C(12), C(13), N(11), O(11)
(2) 0·01 (3) $0{\cdot}446X+0{\cdot}873Y-0{\cdot}199Z=-1{\cdot}16$
Peptide group II: (1) C(13), C(14), C(15), N(12), O(12)
(2) 0·04 (3) $0{\cdot}882X-0{\cdot}268Y+0{\cdot}388Z=5{\cdot}12$

(1) Plane-forming atoms.
(2) R.m.s. displacement (Å) of atoms from the plane.
(3) Equation of the plane. *X*, *Y* and *Z* are along *a*, *b* and *c* and measured in Å.

Table 9. *Interatomic distances less than* 3·6 Å *for* DL-*AANMA*

Between *M* and *M*		Between M_{rev} and M_{rev}	
C(1)···O(1^{i})	3·51 (1) Å	C(12)···C(15^{v})	3·5 Å
C(3)···O(2^{v})	3·57 (1)	C(12)···N(12^{v})	3·5
C(4)···O(2^{v})	3·57 (1)	C(14)···N(12^{v})	3·5
C(6)···O(2^{ii})	3·42 (1)	N(11)···N(12^{v})	3·4
N(2)···C(1^{v})	3·60 (1)	N(11)···C(16^{vi})	3·2
N(2)···C(2^{v})	3·45 (1)	*N(11)···O(11^{v})	2·9
N(2)···N(1^{v})	3·46 (1)	O(11)···C(16^{iii})	3·1
*N(2)···O(2^{v})	2·80 (1)	O(12)···C(13^{v})	3·5
O(1)···C(1^{v})	3·56 (1)	O(12)···C(14^{v})	3·5
*O(1)···N(1^{v})	2·94 (1)	O(12)···C(15^{v})	3·4
		*O(12)···N(12^{v})	2·7

Between *M* and M_{rev}			
C(4)···N(12^{v})	3·50 Å	O(2)····C(16^{iii})	3·27
C(6)···O(11^{ii})	3·30	C(12)···O(1^{v})	3·54
C(6)···O(11^{iv})	3·52	C(13)···O(2^{v})	3·57
C(6)···C(16^{vi})	3·43	C(15)···O(1^{i})	3·51
*N(1)···O(12^{vii})	2·70	C(16)···O(2^{v})	3·54
N(2)···C(15^{v})	3·60	N(11)···N(1^{v})	3·43
N(2)···C(16^{vi})	3·13	*N(11)···O(2^{v})	2·72
N(2)···N(12^{v})	3·27	O(12)···C(1^{v})	3·40
*N(2)···O(11^{v})	2·92	O(12)···C(2^{v})	3·46
O(1)···C(15^{v})	3·56	O(12)···C(3^{v})	3·54
*O(1)···N(12^{v})	2·76	O(12)···C(6^{v})	3·55
O(1)···C(15^{i})	3·51		

(i)	$\frac{1}{2}-x$	$\frac{1}{2}-y$	$\frac{1}{2}-z$	(ii)	$\frac{1}{2}-x$	$-\frac{1}{2}-y$	$\frac{1}{2}-z$
(iii)	$\frac{1}{2}+x$	y	$\frac{1}{2}-z$	(iv)	$-\frac{1}{2}+x$	y	$\frac{1}{2}-z$
(v)	$\frac{1}{4}+y$	$\frac{1}{4}-x$	$\frac{1}{4}+z$	(vi)	$\frac{1}{4}+y$	$-\frac{1}{4}-x$	$\frac{3}{4}-z$
(vii)	$\frac{1}{4}-y$	$-\frac{1}{4}+x$	$-\frac{1}{4}+z$				

* Hydrogen bond.

As already mentioned, the peptide chain of AANMA has a right-hand twist when viewed along the chain. It follows that the β sheet formed by such chains has a left-hand twist when viewed along the axis perpendicular to the peptide chain (Chothia, 1973). Actually, in the crystals of DL- and L-AANMA, the sense of twist of the helical unit composed of L molecules is left handed. The angle of the twist between the neighbouring molecules along the helix axis is exactly 90° in DL-AANMA.

From the above discussion it would not be surprising to find such a strongly twisted sheet structure for the simple peptide molecules, since the AANMA molecule has only two peptide groups available for the formation of hydrogen bonding and even such a large twist as has been observed in the present crystals does not cause too great a distortion of the hydrogen bonds. Table 7 shows the distortions of the hydrogen bonds in AANMA in comparison with those found in related polymers.

The short interatomic distances less than 3·6 Å between the molecules are listed in Tables 9 and 10. Since the atoms in M_{rev} are in the assumed positions, no great significance can be attached to the distances involving M_{rev}.

Table 10. *Interatomic distances less than* 3·6 Å *for* L-*AANMA*

C(1)···O(12^{ii})	3·54 (4) Å
C(2)···O(12^{ii})	3·57 (5)
C(3)···O(11^{i})	3·32 (5)
C(4)···N(12^{i})	3·35 (5)
C(4)···O(11^{i})	3·45 (4)
C(6)···O(12^{ii})	3·51 (4)
C(11)···O(1^{iii})	3·54 (5)
N(1)···N(11^{ii})	3·47 (4)
*N(1)···O(12^{ii})	2·72 (5)
N(2)···C(14^{i})	3·46 (4)
N(2)···N(12^{i})	3·27 (4)
*N(2)···O(11^{i})	2·73 (4)
O(1)···C(13^{i})	3·34 (5)
*O(1)···N(12^{i})	2·80 (3)
*O(2)···N(11^{ii})	2·92 (3)
O(11)···C(16^{iii})	3·32 (3)

(i) $x \quad y \quad z$ (ii) $\frac{1}{2}-x \quad -y \quad \frac{1}{2}+z$
(iii) $\frac{1}{2}+x \quad \frac{1}{2}-y \quad 1-z$

* Hydrogen bond.

The authors wish to express their gratitude to Professors T. Shimanouchi and M. Tsuboi, University of Tokyo, for valuable advice. They also wish to thank Dr Y. Koyama, Kwansei Gakuin University and Dr T. Akimoto, University of Tokyo, for providing us

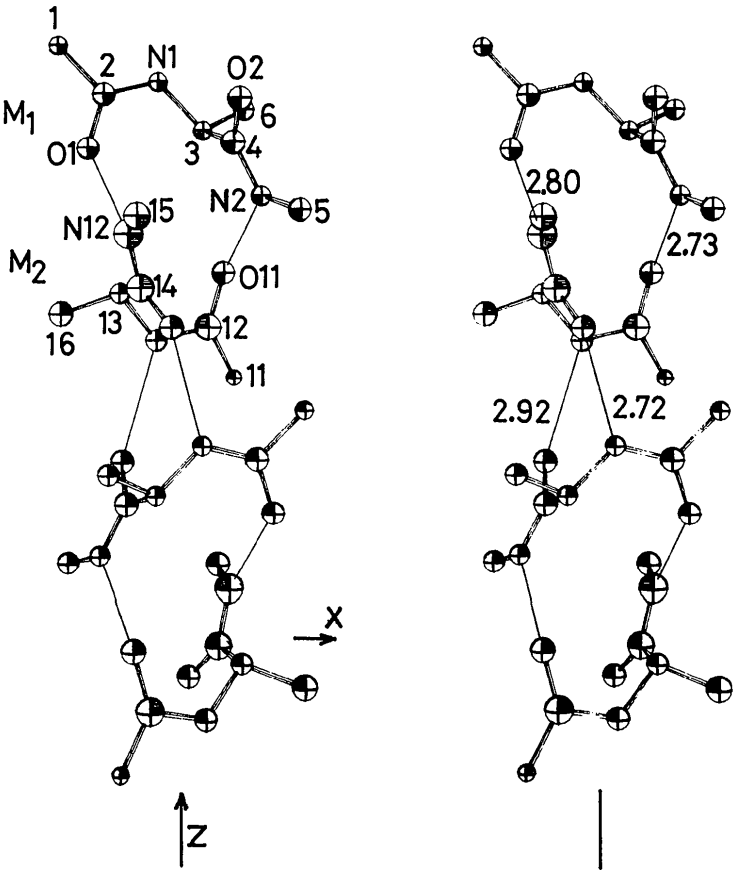

Fig. 6. A stereoscopic drawing of the helical unit found in L-AANMA viewed along the *b* axis. The atoms are drawn by 13% probability ellipsoids. Hydrogen bonds are shown as single thin lines.

with the samples and for many valuable discussions. Thanks are also due to Century Research Center for the use of a CDC 6600 computer.

References

CHOTHIA, C. (1973). *J. Mol. Biol.* **75**, 295–302.
CRICK, F. H. C. & RICH, A. (1955). *Nature, Lond.* **176**, 780–781.
HARADA, Y. & IITAKA, Y. (1974). *Acta Cryst.* B**30**, 726–730.
ICHIKAWA, T. & IITAKA, Y. (1969). *Acta Cryst.* B**25**, 1824–1833.
IWASAKI, F. (1972). *Acta Cryst.* A**28**, S13.
JOHNSON, C. K. (1965). *ORTEP*. Report ORNL-3794, Oak Ridge National Laboratory, Oak Ridge, Tennessee.
KARLE, J. & KARLE, I. L. (1966). *Acta Cryst.* **21**, 849–859.
KOYAMA, Y., SHIMANOUCHI, T., SATO, M. & TATSUNO, T. (1971). *Biopolymers*, **10**, 1059–1074.
MARSH, R. E., COREY, R. B. & PAULING, L. (1955). *Acta Cryst.* **8**, 710–715.
MARSH, R. E. & GLUSKER, J. P. (1961). *Acta Cryst.* **14**, 1110–1116.
PAULING, L. & COREY, R. B. (1951). *Proc. Natl. Acad. Sci. U.S.* **37**, 235–240.
PAULING, L. & COREY, R. B. (1953). *Proc. Natl. Acad. Sci. U.S.* **39**, 253–256.
RAMACHANDRAN, G. N., RAMAKRISHNAN, C. & SASISEKHARAN, V. (1963). *J. Mol. Biol.* **7**, 95–99.
SASISEKHARAN, V. (1962). *Collagen*, edited by N. RAMANATHAN, pp. 39–78. New York: Interscience.

Acta Cryst. (1974). B**30**, 1459

Structure Cristalline de la Phase Type 'Bronze de Ruthénium' $Na_{3-x}Ru_4O_9$

PAR JACQUES DARRIET

Service de Chimie Minérale Structurale de l'Université de Bordeaux I, *associé au CNRS*, 351 *cours de la Libération*, 33405-*Talence, France*

(*Reçu le* 30 *novembre* 1973, *accepté le* 14 *février* 1974)

The $Na_{3-x}Ru_4O_9$ ($x \simeq 0{\cdot}9$) phase crystallizes in the monoclinic system. The space group is $C2/m$, with $a = 23{\cdot}180 \pm 0{\cdot}006$, $b = 2{\cdot}832 \pm 0{\cdot}002$, $c = 10{\cdot}990 \pm 0{\cdot}004$ Å, $\beta = 104{\cdot}50°$. The $[Ru_4O_9]_n^{(3-x)n-}$ network is formed by single, double and triple chains of $[RuO_6]$ octahedra sharing edges. These chains are linked together parallel to the b axis by their corners. The sodium ions are inserted in three different sites in the tunnels.

La synthèse et l'étude structurale de phases oxygénées à base de ruthénium ont été entreprises au laboratoire. Dans le système ternaire sodium–ruthénium–oxygène, de nombreux composés inédits ont été mis en évidence et leurs caractères cristallographiques précisés (Darriet & Galy, 1974; Darriet & Vidal, 1974). C'est ainsi que nous avons mis en évidence, dans le système ternaire Na_2O–RuO_2–'Ru_2O_3', à côté de la phase $NaRu_2O_4$ isotype du ferrite $CaFe_2O_4$, une autre phase originale de formule $Na_{3-x}Ru_4O_9$.

Préparation et données cristallographiques

$Na_{3-x}Ru_4O_9$ était obtenu à partir de mélanges de Na_2RuO_4, de RuO_2 et de ruthénium métallique:

$$(3-x)Na_2RuO_4 + (3+2x)RuO_2 + (2-x)Ru \rightarrow 2Na_{3-x}Ru_4O_9.$$

Les préparations étaient effectuées en tubes scellés d'or, la montée en température se faisant progressivement par paliers successifs à 500 et 600 °C. Le produit de réaction était finalement broyé et maintenu 24 h à 950 °C. La phase $Na_{3-x}Ru_4O_9$ comporte un domaine d'existence correspondant à $0{,}25 \geq x \geq 0$. La poudre bien cristallisée est de couleur bleu acier. Le traitement à 1100 °C de la poudre obtenue pour $x = 0{,}25$ suivi d'un refroidissement lent entraîne la formation de belles aiguilles monocristallines douées d'éclat métallique dont l'axe de croissance correspond à l'axe Oy.

Les diagrammes de Bragg et de Weissenberg ont permis de préciser, pour l'une d'entre elles, les paramètres a, b, c et l'angle β de la maille monoclinique (dimensions: $0{,}08 \times 0{,}01 \times 0{,}02$ mm). Une seule règle d'extinction a été relevée:

$$hkl: h+k = 2n+1.$$

Elle correspond aux groupes spatiaux $C2$, Cm ou $C2/m$. L'ensemble de ces constantes cristallographiques est rassemblé au Tableau 1. Le spectre X de la poudre obtenue après broyage des cristaux a été indexé (Tableau 2).

Tableau 1. *Constantes cristallographiques de* $Na_{3-x}Ru_4O_9$

a	$23{,}180 \pm 0{,}006$ Å
b	$2{,}832 \pm 0{,}002$
c	$10{,}990 \pm 0{,}004$
β	$104{,}50 \pm 0{,}03°$
	$C2/m$
d_{calc}	5,67
Z	4